Insights into deep-sea hydrothermal vent environments from measurements of permeability and porosity

Jill L. Gribbin – Department of Geology, University of Maryland

1 Introduction

Mixing between seawater and vent fluid controls environmental conditions, such as pore fluid temperature, pH, and chemical composition, present at deep-sea hydrothermal vents. However, pore evolution processes, such as mineral precipitation, dissolution, and thermal cracking, modify fluid flow, consequently influencing environmental conditions. Also, biological communities living at vent fields depend on the fluid flow for nourishment, making it even more critical to understand fluid flow properties. Studying the permeability and porosity of vent deposits can provide much needed information on fluid flow. Permeability (*k*) is the ability of a material to transmit fluid, whereas porosity is the fraction of void space in a given volume. Measurements of these vent properties determine the evolution of permeability-porosity relationships (EPPRs) that provide valuable insight into the magnitude and direction of fluid flow in vent deposits.

Hypothesis: Vent deposits from mid-ocean ridges around the world will display distinguishable permeability-porosity evolution trends.

2 Samples

This study examined five different types of vent deposit samples from hydrothermal fields around the world:

- **Massive anhydrite** – produced from the precipitation of $CaSO_4(s)$ as seawater is entrained into vent deposit mounds, mixes with hot vent fluid, and is heated conductively (8 samples from 3 vent fields)
- **Flanges / slabs / crust** – evolve as pooled fluids percolate upward through ledges composed of sulfide, sulfate, and/or carbonate (10 samples from 4 vent fields)
- **Black smoker chimneys** – develop around jets of high-temperature metal- and sulfide-rich fluid in two stages: (1) anhydrite precipitation from seawater / fluid mixing, (2) sulfide mineral precipitation along inner central conduit lining and in pore spaces within the anhydrite wall (8 samples from 4 vent fields)
- **Zn-rich diffusing spire** – formed from lower-temperature (<300 to 330°C), less vigorously venting fluid; vent fluid percolates through mm-sized anastomosing channels, forming porous spires that lack an open central conduit (7 samples from 4 vent fields)
- **Relict spires** – spires that were not actively venting when recovered, presumably because flow ceased after passages were blocked by mineral precipitation (6 samples from 5 vent fields)

Flange

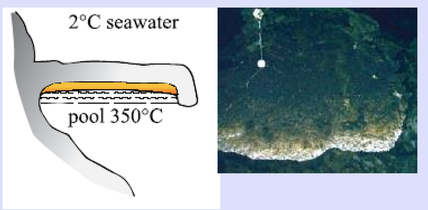

Black Smoker

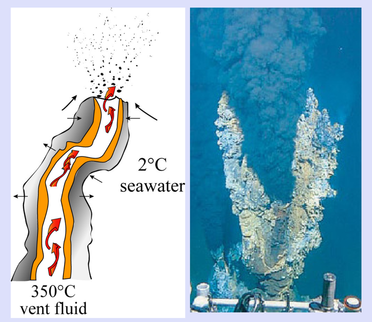

Diffusing Spire

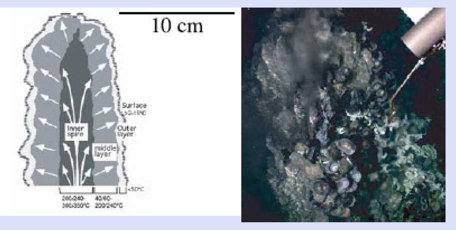

Images from Tivey (2007)

3 Procedure

- Make permeability measurements using a portable probe permeameter (NER TinyPerm™) on different surfaces of samples with several sites per surface type, and five measurements per site.
- Cut multiple cylindrical cores for each sample in varying directions, all with a 2.5 cm diameter, and seal cores in plastic.
- Take directional permeability using a N_2-permeameter (Ultraperm™400) and porosity measurements with a He-porosimeter (UltraPore™300).
- Make sample thin sections and perform petrographic analysis of mineral processes

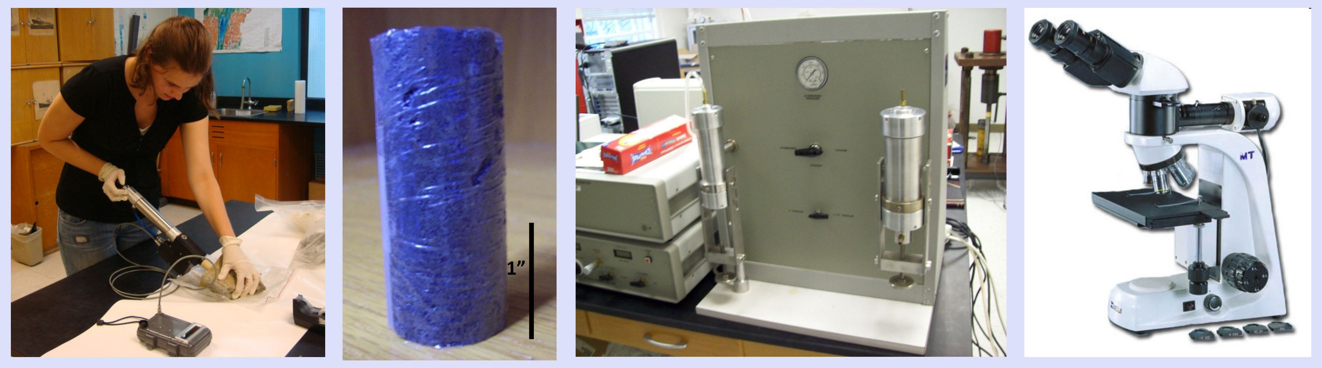

4 Probe Permeameter

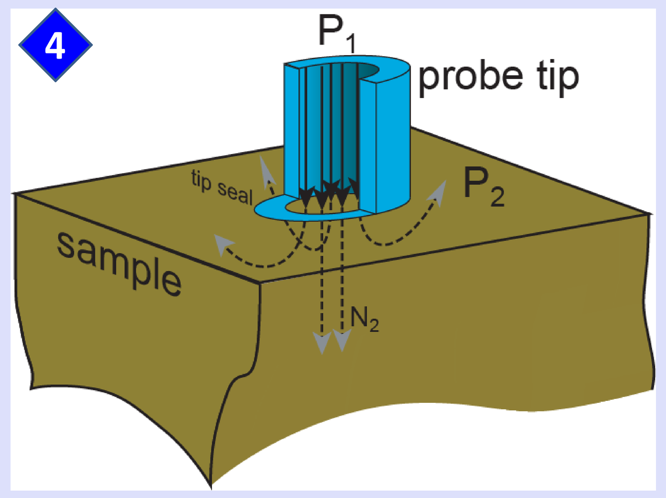

The probe permeameter measures gas flow into a porous medium through a rubber tip that forms an air-tight seal against the surface of the sample. Using Darcy's Law, the gas flow rate is converted to permeability, *k*.

$$q = \frac{k(\Delta P)}{\mu L}$$

q = flow rate; ΔP = pressure gradient; μ = gas viscosity; L = sample length

Permeability Ranges:

Massive anhydrite ≈ $1 \times 10^{-14} – 6 \times 10^{-12}$ m^2
Flanges/slabs/crust ≈ $6 \times 10^{-14} – 2 \times 10^{-10}$ m^2
Black smokers ≈ $2 \times 10^{-14} – 8 \times 10^{-11}$ m^2
Diffusing spires ≈ $6 \times 10^{-13} – 8 \times 10^{-10}$ m^2
Relict spires ≈ $4 \times 10^{-14} – 2 \times 10^{-10}$ m^2

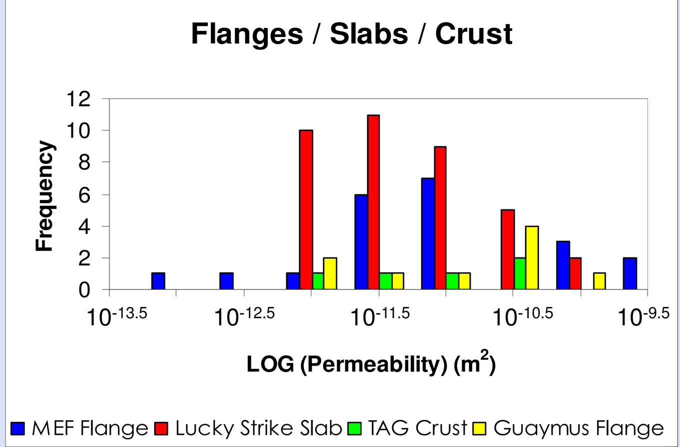

Largest *k* range

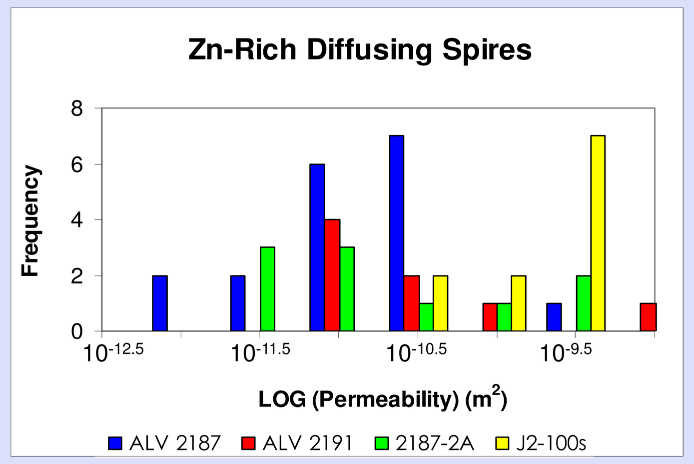

Highest *k* values

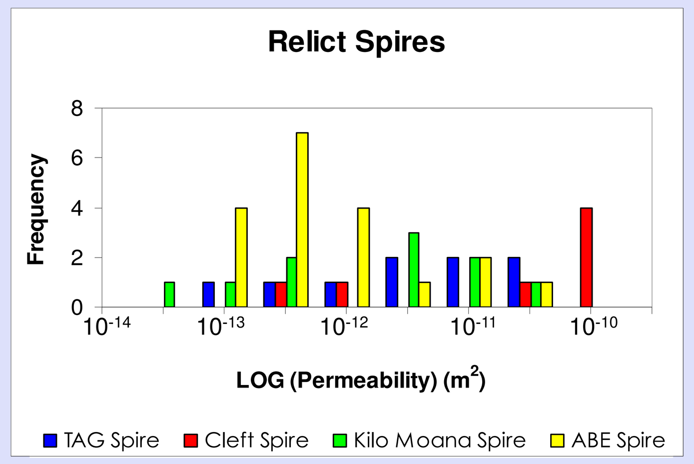

Display anisotropy – lower *k* in axial direction and higher *k* in radial direction

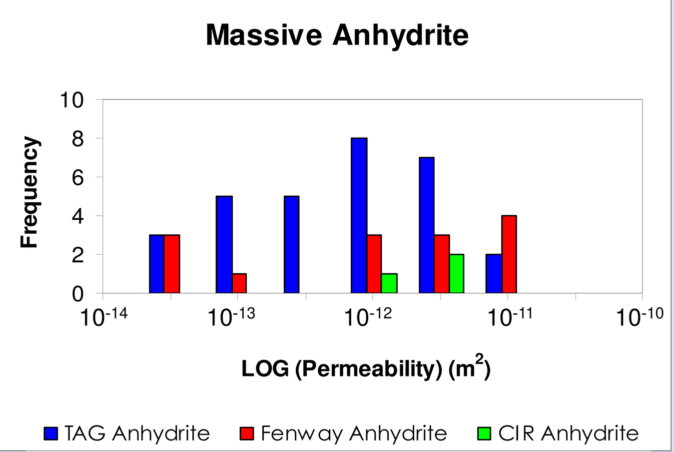

Lowest *k* values

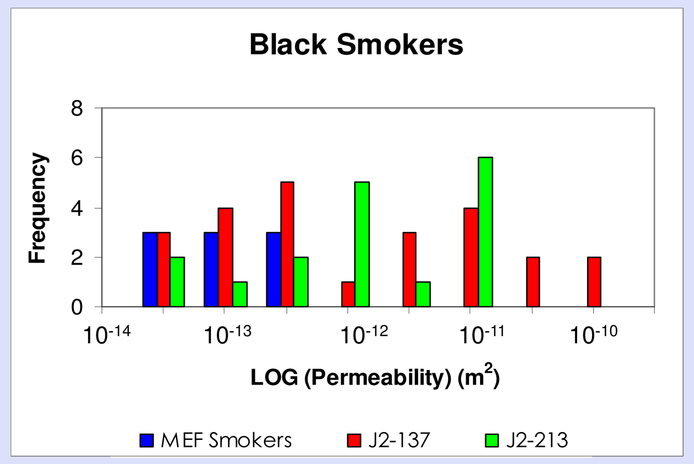

Show layered heterogeneity – lower *k* along inner lining and higher *k* outwards

5 Vent Deposit Permeability

Directional permeability from the relict spire, massive anhydrite, and flange / slab / crust groups. Average core permeability for the samples is plotted against the applied confining pressure (plots include probe permeameter measurements)

Fenway Anhydrite: J2-210-8-R2

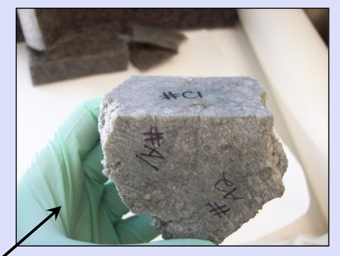

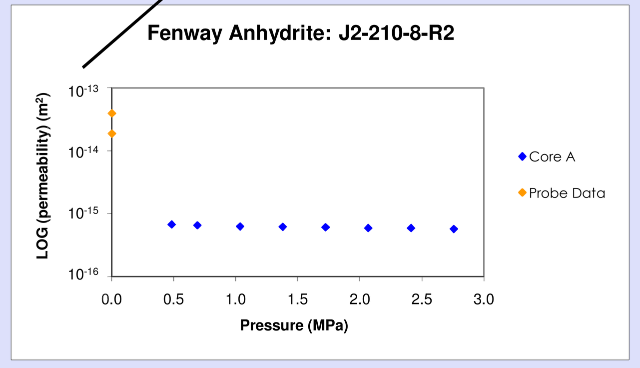

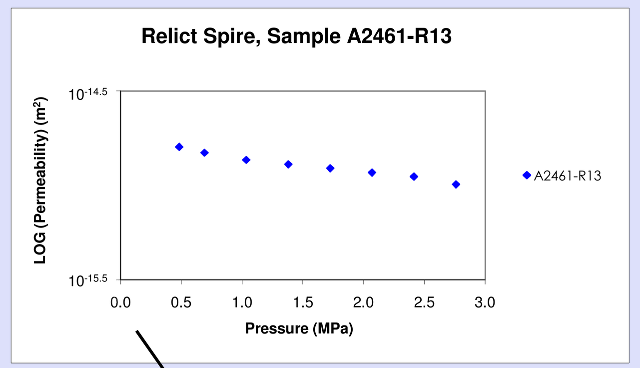

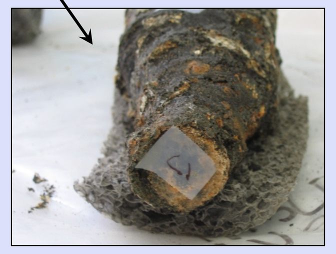

Relict Spire: A2461-R13

MEF Flange: 2927

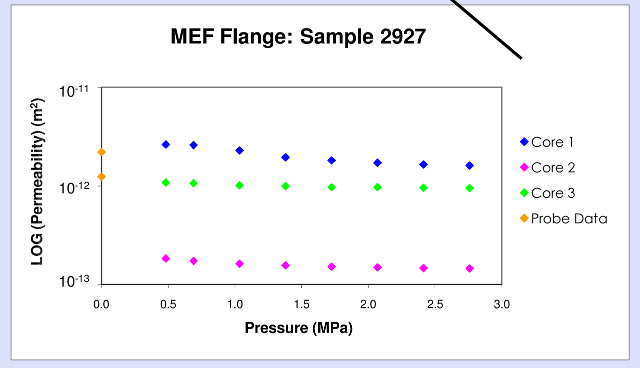

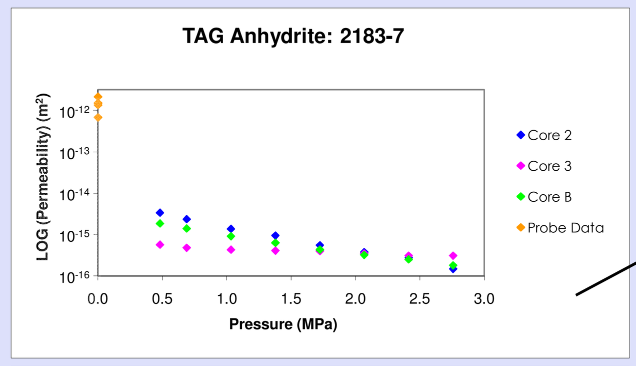

TAG Anhydrite: 2183-7

MEF Flange: 2415-1B

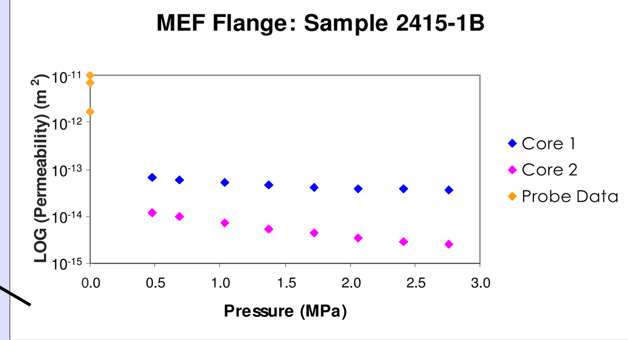

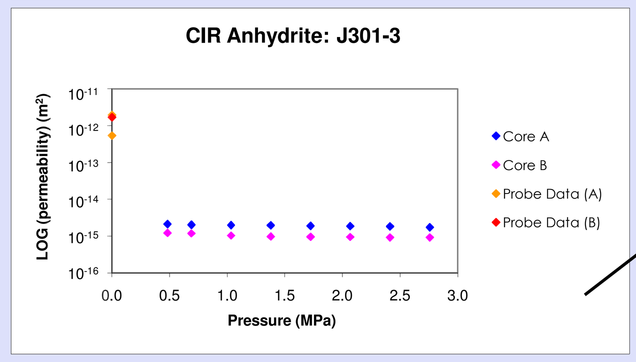

CIR Anhydrite: J301-3

Lucky Strike Slab: 2608-4

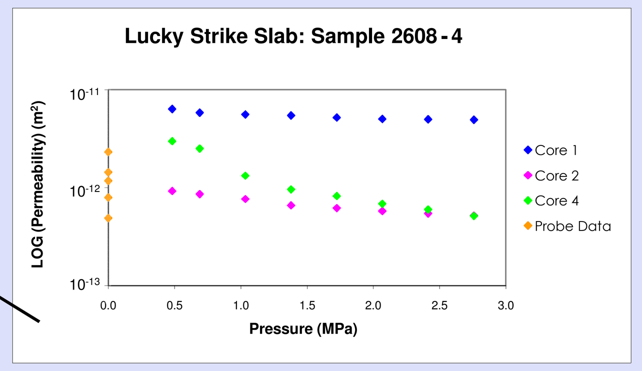

6 Permeability – Porosity Relationships

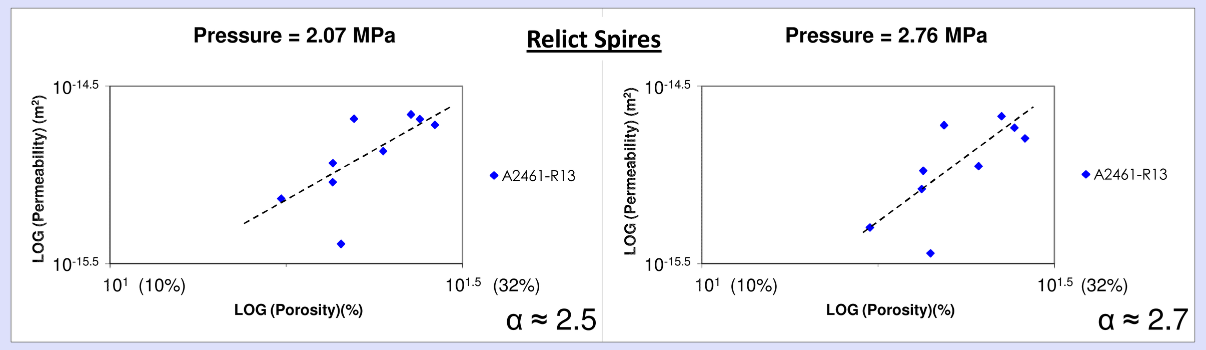

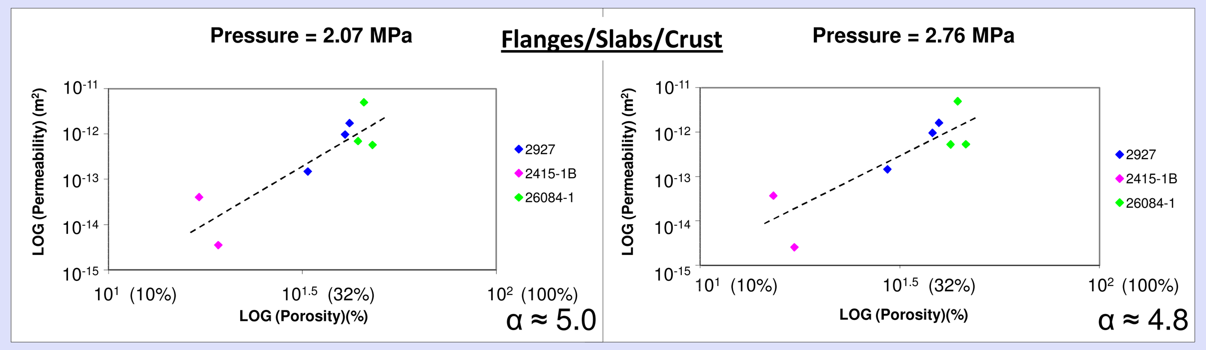

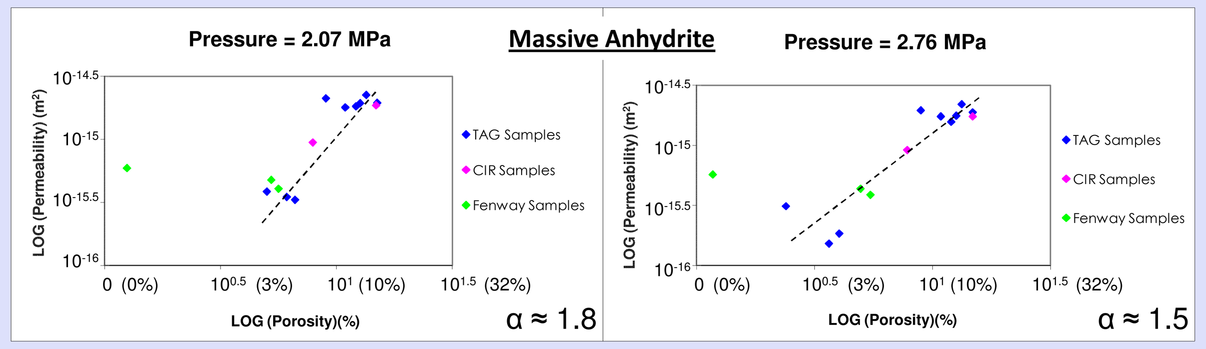

Porosity data from the He-porosimeter can be plotted against permeability data to find an empirical power- law relationship, with the characteristic exponent, α.

$$\left(\frac{k}{k_0}\right) \propto \left(\frac{\varphi}{\varphi_0}\right)^{\alpha}$$

Resulting α values:
Relict spires ≈ 2.5
Flanges/slabs/crust ≈ 5.0
Massive anhydrite ≈ 1.5

7 Mineral Analysis

Sample: 1A2_3#8

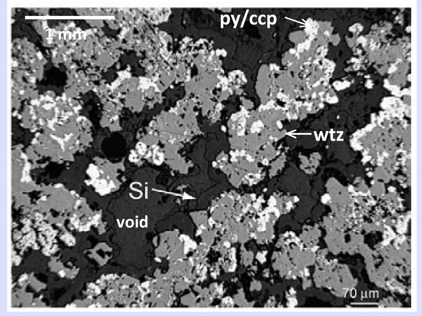

Sample: RnB_#10

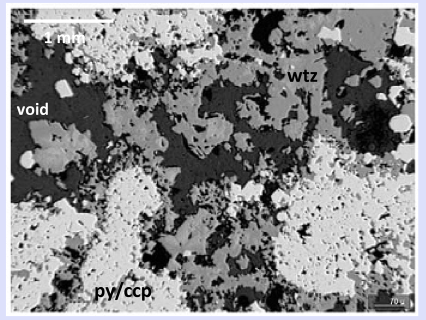

Sample: ALV2-1/78-3-1A

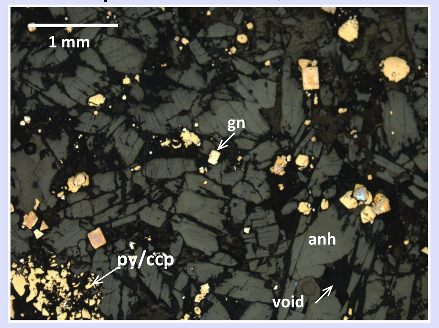

Si = amorphous silica, py = pyrite, ccp = chalcopyrite, wtz = wurtzite, anh = anhydrite, gn = galena, void = void space

Reflected light photomicrographs showing relative proportions of sulfides, sulfates, and void space, which all affect obtained α values.

Relict Spires: Presence of amorphous silica may support α ≈ 2.5, based on Zhu et al. (2007), which found α ≈ 3 for dominant precipitation of amorphous silica, although mineral precipitation varies highly with vent location due to fluid pH resulting in different mineral abudances.

Flanges / Slabs / Crust: Inconsistent presence of amorphous silica; sulfides (pyrite, chalcopyrite, and wurtzite) regularly present. Moderate precipitation of both amorphous silica and various sulfides may account for α ≈ 5, since Zhu et al. (2007) found dominant sulfide precipitation to yield α ≈ 9.

Massive Anhydrite: No amorphous silica present; mostly precipitated anhydrite; minimal pore space due to close grain packing and sulfide infill of pores. Low α value may be representative of anhydrite dominance.

*Additional petrographic analysis is necessary for the samples to obtain a more thorough understanding of the mineral processes present and whether location specific trends exist.

8 Acknowledgments

Many thanks to my advisors: Wen-lu Zhu (UMD) & Margaret Tivey (WHOI)

Also, like to thank Margaret Sulanowska (WHOI), Tommy Tamarkin (UMD), and Sarah Penniston-Dorland (UMD) for their help.

I would additionally like to acknowledge the following grants:

NSF OCE – 0648337 (WHOI)   NSF EAR – 0741339 (UMD)